J Mater Sci (2009) 44:2016–2020
DOI 10.1007/s10853-009-3244-y

Nanoscale ripples on the compressive fracture surface of a bulk metallic glass with microscale crystals

W. Z. Liang · X. Y. Mao · L. Z. Wu · H. J. Yu · L. Zhang

Received: 10 June 2008 / Accepted: 5 January 2009 / Published online: 18 February 2009

Abstract Some periodic and straight strips with about 60 nm spacing were observed on the compressive fracture surface of $Ni_{42}Cu_5Ti_{20}Zr_{21.5}Al_8Si_{3.5}$ bulk metallic glass (BMG) rods containing minor microscale crystals. The characteristic difference between amorphous matrix and microscale crystals also reveal why periodic corrugations could not be observed on the fracture surface of metal crystals. The dynamic crack instability may be explained by the interaction of the propagating crack and the internal micro-cracks. This kind of periodic morphologies showed in-plane feature, which may be attributed to the non-intense interaction between dynamic crack and micro-crack.

Introduction

The dynamic fracture of brittle amorphous material has been an important topic, which people carried out large amount of experimental and theoretical investigations using soda-lime and polyacrylamide, confirming the validity of the continuum theory of dynamic brittle fracture for fast cracks [1, 2]. However, the physical origin of the formation of the periodic strips on the fracture surface is still unclear [3, 4]. The interactions between dynamic crack and elastic waves became the focus of the dynamic fracture domain. Some investigations [5–7] indicated that the reflected elastic waves interacted with crack front, resulting in the instantaneous fluctuation of the stress at the crack's tip. So, the crack periodically propagated and left the periodic marks on the fracture surface. Other studies [8, 9] suggested that crack front underwent an oscillating behavior due to a similar reproducible sequence of instabilities, which intensely depended on both geometric and loading conditions. An experiment showed that Wallner lines were produced by the interaction of external shear waves and propagating cracks [10], and crack front interacting with internal micro-cracks induced the formation of the crack front waves [11]. Recently, Xi et al. [12] and Wang et al. [4]observed periodic marks with a wavelength of 100 nm and 60 nm, on the fracture surfaces of an ideally brittle $Mg_{65}Cu_{25}Ta_{10}$ and $Mg_{65}Cu_{25}Gd_{10}$ metallic glass subjected to three-point bending, respectively. Xi thought that the self-assembly of nanovoids led to the formation of periodic strips under periodic elastic stress field. Wang indicated that the local softening mechanism in the fracture was a key factor for the formation of unique corrugations. Zhang et al. [13] claimed that formation of the periodic nanoscale steps is one of typical cleavage fracture features in the brittle metallic glass. Our previous study on the periodic ripples described reflected periodic marks with spacing of 60 nm on the compressive fracture surface of a 0.5% plastic $Ni_{42}Cu_5Ti_{20}Zr_{21.5}Al_8Si_{3.5}$ BMG rod with diameter of 2 mm [14]. We considered that drastic interaction between dynamic cracks and internal micro-cracks induced the appearance of the periodic strips on the fracture surface. The above analysis suggested that dynamic fracture mechanisms of amorphous materials exhibited large discrepancy, and need to be investigated deeply.

The studies on the dynamic fracture and periodic morphologies were usually focused on the non-metallic glasses with pre-existed cracks in Mode I(tension). In contrast to

W. Z. Liang (✉) · X. Y. Mao
School of Materials Science and Engineering, Heilongjiang Institute of Science and Technology, Harbin 150027, China
e-mail: wzliang1966@126.com

W. Z. Liang · L. Z. Wu · H. J. Yu · L. Zhang
Center for Composite Materials, Harbin Institute of Technology, Harbin 150001, China

the previous close-to-ideal brittle non-metallic glasses plate, in this article, we presented the in-plane periodic marks with spacing of 60 nm formed on the non-shear compressive surface of a $Ni_{42}Cu_5Ti_{20}Zr_{21.5}Al_8Si_{3.5}$ brittle BMG rod containing minor microscale crystals. The formation mechanism of the nanoscale periodic strips and the effect of microscale crystals on the crack propagating were explored on the basis of experimental observations and theoretical analyses.

Experimental procedure

Button ingots of $Ni_{42}Cu_5Ti_{20}Zr_{21.5}Al_8Si_{3.5}$ alloys were fabricated by arc melting of mixtures of the composite element (99.9% purity) in a Ti-gettered argon atmosphere. BMG rod with a diameter of 3 mm and a length of 40 mm was synthesized by casting into a copper mold in a purified argon atmosphere. The structure was charactered by X-ray diffraction (XRD) with Cu-Kα radiation ($\lambda = 1.5405$ Å) using a D/MAX-RB diffractometer and transmission electron microscopy (TEM). Compression tests were performed on 3-mm diameter and 6-mm long cylindrical rods by using an INSTRON-5569 testing machine with a strain rate of 3×10^{-4} s^{-1}. The newly fractured specimen surface was observed in a FEI Sirion high-resolution scanning electron microscope (HRSEM) with a resolution of 1.5 nm, and an AUTOPROBE cp atomic force microscopy (AFM) with a horizontal resolution of 0.25 Å.

Results and discussions

Amorphous alloy microstructure

To explore the distinctive effect of $Ni_{42}Cu_5Ti_{20}Zr_{21.5}Al_8Si_{3.5}$ alloy microstructure on the compressive fracture feature, the microstructure of the Ni-based material must be investigated first. Figure 1 presents XRD curve of the study alloy with a faint Bragg peak(pointed by arrow) on mainly broad maxima, which is indicative of containing minor crystals. TEM observation was conducted to further prove the presence of minor crystals in the BMG, as shown in Fig. 2. It is evident that a sphere-like crystal (Fig. 2b) embeded in amorphous matrix (Fig. 2a), which is also indicated by the inset SAED pattern, is consistent with a few barely visible peaks on the XRD curve.

Compressive fracture feature

To study the effect of spherocrystals structure on the fracture features, we carried out compressive tests on the $Ni_{42}Cu_5Ti_{20}Zr_{21.5}Al_8Si_{3.5}$ BMG rods containing minor

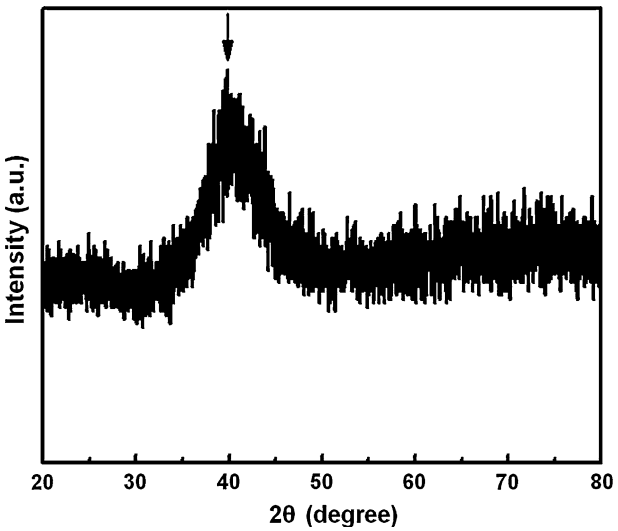

Fig. 1 XRD pattern for $Ni_{42}Cu_5Ti_{20}Zr_{21.5}Al_8Si_{3.5}$ BMG rod containing minor crystals

microscale crystals. Figure 3a exhibits compressive stress–strain curve with only perfectly elastic deformation of the Ni-based alloy, suggesting completely brittle fracture characteristic. Figure 3b shows the side-view of the compressive fracture surface consisting of flat shear zone(I) and scraggly rough zone (II). This revealed that the sample fractured initially in a pure shear mode(zone I), which is characterized by a well-defined fracture angle of 41.8° as well as evenly distributed fishbone-like vein structure (inset in Fig. 3b), followed by a non-shear mode instantaneous failure (zone II). Figure 3c displays the top-view of the fracture surface. This clearly exhibited the bifurcation appearing in main crack propagation, indicating that the crack velocity exceeded a certain limit. The BMG tension feature of radiating veins with round core was observed in the roughing zone(II) (Fig. 3c), indicating the normal tensile stress played an important role in compressive fracture process [15]. The amplified image of the circle sign in Fig. 3c, as shown in Fig. 3d, presents the periodic changes of crack branching, healing, and re-branching along its propagation direction. The periodic evolution of the cracks reflects the fluctuations in the velocities and energies of the crack propagation fronts. This state was similar with the periodic crack propagation band that appeared in previous computational simulation of brittle amorphous polymer dynamic fracture [7].

We further examined the sites of A, B, and C in Fig. 3d under high-resolution SEM and discovered the microscopic fracture feature containing roughness region, transition region, and smooth region along the crack propagation direction, as shown in Fig. 4a, b, and c, respectively. The roughness region (A) was made up of microscale dimples (Fig. 4a). The formation of microvoids indicated that crack

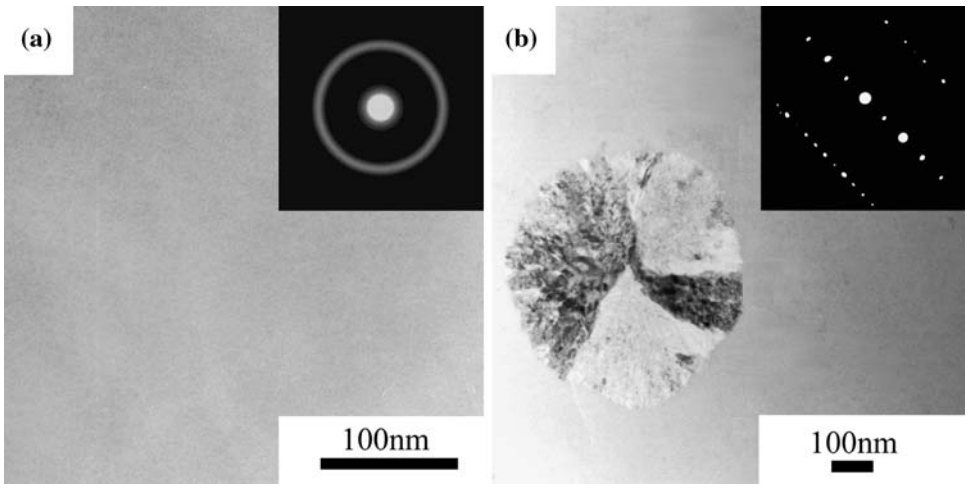

Fig. 2 TEM image and corresponding SAED pattern of a $Ni_{42}Cu_5Ti_{20}Zr_{21.5}Al_8Si_{3.5}$ BMG rod with a diameter of 3 mm. **a** Amorphous matrix, **b** a sphere-like crystal

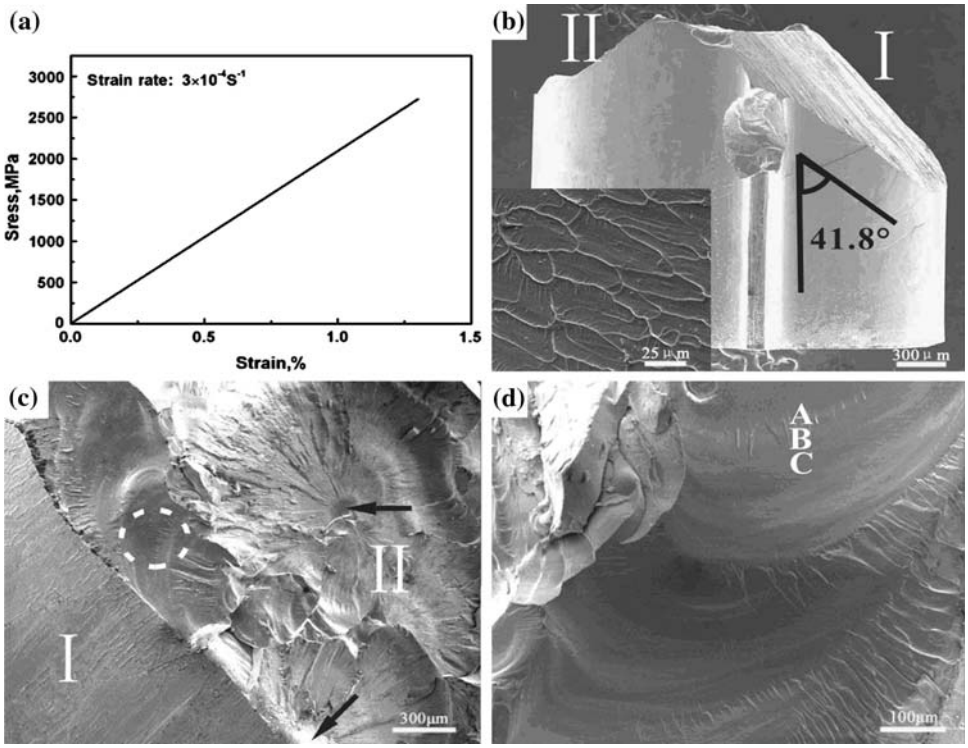

Fig. 3 Compressive fracture characteristic of a $Ni_{42}Cu_5Ti_{20}Zr_{21.5}Al_8Si_{3.5}$ BMG rod with a diameter of 3 mm. **a** The stress–strain curve only showing elastic deformation **b** SEM image showing the side-view of the fracture specimen with a sketch of fracture angle: two zones are labeled. Inset is the top-view of zone I. **c** SEM image showing the top-view of the fracture surface. Arrows point the flower-like structure. **d** SEM image showing the fracture surface for the area as circle in **c**

tip was subjected to large normal tensile stress under compressive load, and dynamic crack propagated through linkage and coalescence of numerous microscale dimple structures [7, 12]. For site B, fracture surface presented the transition region between dimple structures and well-defined periodic wave patterns, which consisted of primary periodic strips and crack branches (Fig. 4b). The crack branches included some well-aligned micro-cracks which aligned along the straight lines parallel to the crack propagation direction. However, when the propagating cracks met with macroscale crystals, the crack branches deviated an angle from the straight line and lost its stability, as indicated by arrows in Fig. 4b. In the meantime, the periodic strips passing the crystals disappeared. This suggested that the microstructure of the materials distinctly effected on the compressive fracture feature [16]. In other words, the sphericity crystal structure that pre-existed in as-cast rod changed the crack propagating path, resulting in the confusional state of crack propagation. This may explain why no periodic morphologies appear on the fracture surface of the ordinary metal crystal structures. A 1 × 1 μm top-view AFM image of the crystal in Fig. 4b, as shown in Fig. 5a, clearly revealed the irregular crack propagation path.

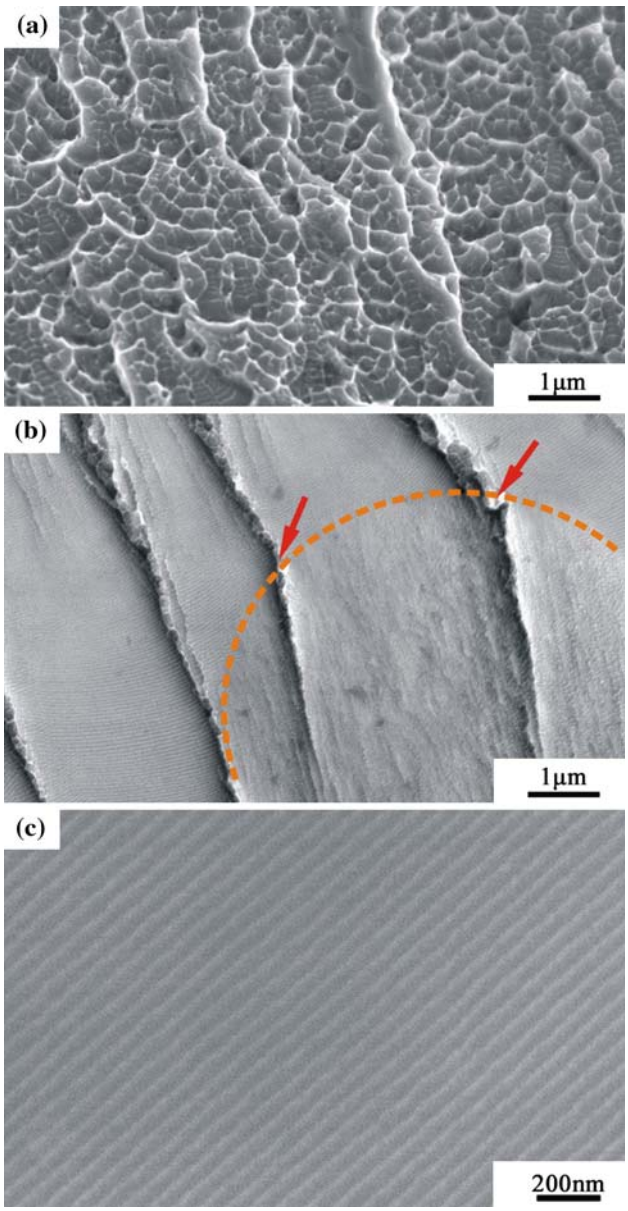

Fig. 4 SEM image showing the fracture surface at high magnifications. **a**, **b**, and **c**, details corresponding to the site, as marked in Fig. 3d by A, B, and C, respectively. The arrows in (**b**) indicate the crystal

The primary periodic wave patterns in transition region developed along the main crack propagation direction to form a largely extended smooth region, as shown in Fig. 4c. It may be seen that wave patterns with nearly constant period are straight and parallel, the average spacing is about 60 nm. This implies that the crack velocity changes slowly and the whole crack front is straight [12]. The structure details of the strips are further displayed in a 1 × 1 μm AFM top-view image (Fig. 5b), and the inset (Fig. 5c) presents the amplitude changes of the periodic wave patterns on the fracture surface. It can be seen that the wavelength of ripples is also about 60 nm and the average

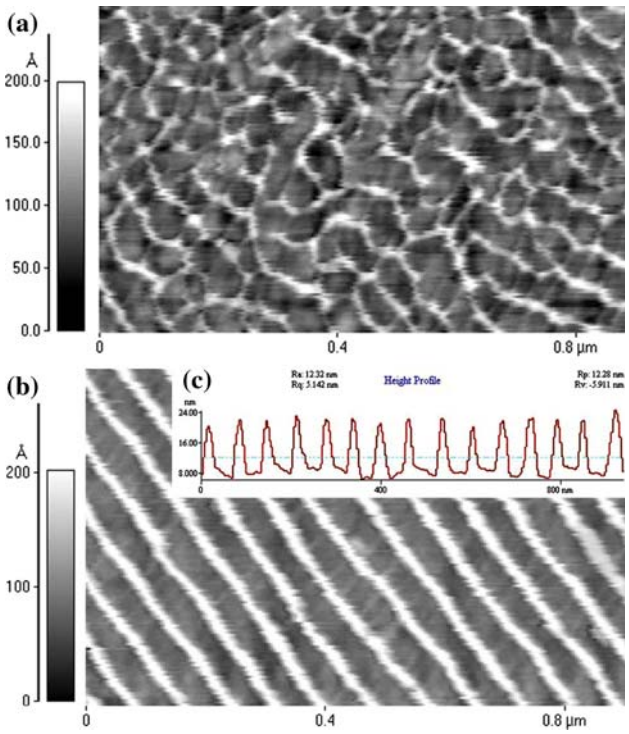

Fig. 5 AFM top-view images in 1 × 1 μm. **a** The crystal in Fig. 4b. **b** Periodic marks in Fig. 4c. **c** Averaged profile of the periodic marks in **b**

amplitude is approximately 4 nm, which revealed the in-plane feature of the nanoscale wave pattern propagation.

The nanoscale periodic marks on the fracture surface are generated by the interaction between the dynamic crack and intrinsic formation of micro-cracks. Some experiments [1, 17] showed that beyond a critical velocity ($\approx 0.4 v_R$), dynamic crack underwent a repetitive process of micro-branching events, leading to large oscillations in the crack velocity and the formation of periodic corrugations along a branch line. Due to the limited experimental condition, we could not measure the critical velocity of $Ni_{42}Ti_{19}Zr_{22.5}Al_8Cu_5Si_{3.5}$ BMG rod in compression. However, the universal nature of the micro-branching instability has been demonstrated and the appearance and evolution of the instability on fracture surface are nearly identical [1]. It can be proved by the transition from flat shear zone (I) to rough zone (II) and the appearance of periodic wave pattern along the branch line (Fig. 4b). This implies that the appearance of microbranch is related to the formation of periodic ripples. How do the intrinsic micro-cracks generate in metallic glass? Micro-cracks first nucleated at a site, such as inherent atomic density fluctuation and free volume in the metallic glasses [18], in front of the crack during deformation. The crack nucleus may grow under continuous straining [19], and is eventually connected to form a continuous fracture path. The well-aligned microcracks ahead of the crack front induced new energy fluctuation,

which created the periodic pulses persisting in the velocity of the crack front [20]. The persistence of velocity fluctuation represented periodic strips on the fracture surface containing a large amount of plastic dimples. This may be proved by the AFM pattern embodying the amplitude change (Fig. 5c). From the point of consuming energy, the existence of many dimples may help to increase the instability of the main crack propagation and induce the formation of micro-cracks [21]. Therefore, the early-stage wave patterns formed and propagated along the micro-branch lines (Fig. 4b and c).

Conclusions

We observed periodic marking with spacing of about 60 nm on the compressive fracture surface of $Ni_{42}Cu_5Ti_{20}Zr_{21.5}Al_8Si_{3.5}$ BMG rod containing minor microscale crystals. This effects the interactions between dynamic crack front and local micro-cracks. The existence of sphericity crystal clearly demonstrates the dynamic crack propagation and confusional path in the fracture process of the ordinary crystal structure.

Acknowledgements The authors gratefully acknowledge the financial support by the Program for Heilongjiang Institute of Science and Technology Excellent Talents (07–57), the Foundation of China Postdoctor (20070420871), as well as Heilongjiang Province Postdoctor (AUGA41001081). This study was also supported by Foundation of education office of Heilongjiang Province under Project No.11531316, and the Foundation of Heilongjiang Nature Science (A200808).

References

1. Sharon E, Fineberg J (1999) Nature 397:333
2. Bonamy D, Ravi-Chandar K (2003) Phys Rev Lett 91:235502
3. Sharon E, Cohen G, Fineberg J (2001) Nature 410:68
4. Wang G, Zhao DQ, Bai HY et al (2007) Phys Rev Lett 98:235501
5. Tran Nguyen H, Lamb Robert N (2004) Chem Phys Lett 391:385
6. Fitzgerald AM, Kenny TW, Dauskardt RH (2003) Exp Mech 43:317
7. Ravi-Chandar K, Yang B (1997) J Mech Phys Solids 45:535
8. Marlière C, Despetis F, Phalippou J (2003) J Non-Cryst Solids 316:21
9. Adda-Bedia M, Ben Amar M (1996) Phys Rev Lett 76:1497
10. Sharon E, Cohen G, Fineberg J (2002) Phys Rev Lett 88:085503
11. Fineberg J, Gross SP, Marder M et al (1991) Phys Rev Lett 67:457
12. Xi XK, Zhao DQ, Pan MX et al (2005) Phys Rev Lett 94:125510
13. Zhang ZF, Wu FF, Gao W et al (2006) Appl Phys Lett 89:251917
14. Shen J, Liang WZ, Sun JF (2006) Appl Phys Lett 89:121908
15. Zhang ZF, He G, Eckert J et al (2003) Phys Rev Lett 91:045505
16. Ravi-Chandar K, Knauss WG (1984) Int J Fract 26:141
17. Livne A, Cohen G, Fineberg J (2005) Phys Rev Lett 94:224301
18. Inoue A (2000) Acta Mater 48:279
19. Pan DG, Zhang HF, Wang AM et al (2006) J Alloys Compd 438:145
20. Morrissey JW, Rice JR (1998) J Mech Phys Solids 46:467
21. Sharon E, Fineberg J (1999) Advanced Eng Mater 1:119